Ge Baoming, Wang Xiangheng, Jiang Jingping

Nonlinear Internal-Model Control for Switched Reluctance Drive with Torque Ripple-Free

Based on the nonlinear internal-model control (IMC), associated with the suitable commutation strategy, a novel control solution for switched reluctance motor (SRM) is formulated and designed. The commutation strategy uses a definite critical rotor position as commutation point, which reduces the computational burden. The nonlinear IMC-based voltage control scheme for SRM extracts the simplicity of the feedback linearization control and the robustness of IMC structure, which ensures the torque ripple-free and the drive's robustness in spite of the plant--model mismatch disturbances. Some important properties are presented. Simulation results show that the high-performance control for SRM has been achieved.

Key words: nonlinear internal-model control, SRM, torque-ripple minimization

1 INTRODUCTION

Switched reluctance motor (SRM) drives are suitable for many variable speed and servo type application, and gaining increasing attention in the motor drive industry. However, the SRM presents a coupled nonlinear multivariable control structure, early classical linear controllers are not fast enough to take into account the nonlinearity of the SRM electromagnetic characteristics, which results in ripples in the torque profile [1, 2]. The drawback has led to a search for complex nonlinear control methods to compensate for the machine nonlinearity and torque ripples.

One approach that has been investigated most extensively is the feedback linearization control (FLC) [3–6]. The application of this technique is simple and straightforward, but it needs an accurate model. Using an approximate model does not produce a linear closed-loop system, and the performance of the SRM drives degraded, in some cases even led to an unstable response.

Nonlinear internal-model control (IMC) combines the simplicity of FLC technique and the robustness of IMC structure [7, 8]. The control system is not only highly robust with respect to modeling uncertainties and to other kinds of disturbances, but also can effectively compensate for the nonlinearity of the plant. The nonlinear IMC implicitly includes integral action, and can guarantee the convergence of the plant output to a steady state constant reference. Although the nonlinear IMC displays so many interesting properties, as far

as the authors are aware, it has not yet applied to the SRM drives.

In this paper, based on the nonlinear IMC, associated with a suitable commutation strategy, a novel control solution for SRM is formulated and designed, which ensures the torque ripple-free and robustness in spite of the plant-model mismatch or disturbances.

2 COMMUTATION STRATEGY

In general, the single-phase conduction commutation strategy is widely used due to its simpleness, and but it does not essentially meet the expectation of the torque ripple-free owing to its resulting in the phase voltage saturation. Therefore, it is important to propose a suitable commutation strategy to compensate for the effects of the saturation.

As shown in Figure 1, θ_c is defined as a commutation point, which is periodic with period $\theta_p = 2\pi/mN_r$ where m and N_r are the numbers of stator phases and rotor poles, respectively. Due to the finite inverter voltage, the commutation process cannot be instantaneous. So the on-coming phase-b be excited at an advancing angle θ_{on}. Thus, the phase conduction region is divided into two sections, namely $\theta_{on} \leq \theta \leq \theta_c$ and $\theta_c \leq \theta \leq \theta_c + \theta_P$, respectively. From θ_{on} to θ_c, phase-a is the stronger phase, which is the main torque contributor, and the flux linkage in phase-b must be driven from zero as rapidly as possible. During this period, the controller forces the entire inverter voltage to be applied to phase-b in
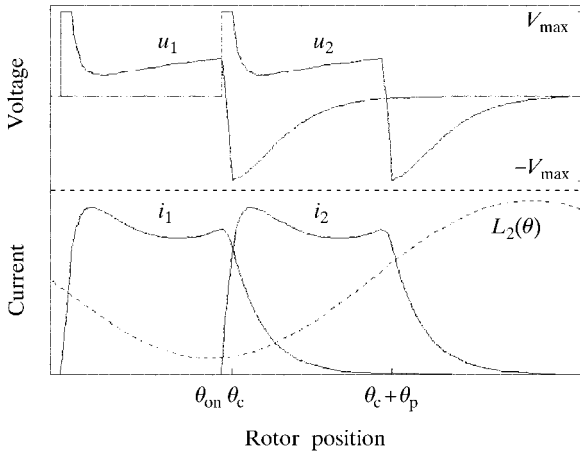
Fig. 1 Novel commutation scheme

order to minimize the magnetization periods. Meanwhile, the applied voltage for phase-a is calculated in real time taking into consideration the actual torque developed by the phase-b so that the desired total torque can be produced. As θ moves past θ_c, phase-a is no longer the main torque producer, and it should be demagnetized quickly as possible, while the current in phase-b, which is now stronger, becomes the main torque contributor up to $\theta_c + \theta_P$.

Remarks: Compared with the commutation strategies in [9] and [10], although there exist certain similitude in the one proposed by the present paper, but the following distictions are obvious:

a) In [9] and [10], the critical rotor positions θ_c will change when the required torque changes. In our commutation strategy, it is invariable in any case.

b) During the demagnetization period, unlike the approach reported in [9] where $di/d\theta$ was fixed, and also unlike in [10] where $d\psi/d\theta = -V_{max}/\omega$. In our commutation strategy, $di/d\theta$ is controlled by the nonlinear IMC.

c) Turn-off angle θ_{off} is not required in our commutation strategy.

3 NONLINEAR IMC OF SRM

3.1 Electrical dynamic model

When the plant output is the total torque that is to be controlled to the desired reference, the electrical dynamic model based on the novel commutation strategy can be deduced as:

$$\begin{cases} \dfrac{dT_e^M}{dt} = F_{k1}^M + G_{k1}^M u_{k1} \\ y_{Te}^M = T_e^M \end{cases} \tag{1}$$

$$\begin{cases} \dfrac{di_{k2}^M}{dt} = f_{k2}^M + g_{k2}^M u_{k2} \\ y_{k2}^M = i_{k2}^M \end{cases} \tag{2}$$

$$\begin{cases} \dfrac{di_f^M}{dt} = f_f^M + g_f^M u_f \\ y_f^M = i_f^M \end{cases} \tag{3}$$

with

$$F_{k1}^M = -\frac{\partial T_{k1}^M}{\partial i_{k1}^M} \cdot \left(\frac{\partial \psi_{k1}^M}{\partial i_{k1}^M}\right)^{-1} \cdot \left(R^M i_{k1}^M + \frac{\partial \psi_{k1}^M}{\partial \theta}\omega\right) -$$
$$- \frac{\partial T_{k2}^M}{\partial i_{k2}^M} \cdot \left(\frac{\partial \psi_{k2}^M}{\partial i_{k2}^M}\right)^{-1} \cdot \left(R^M i_{k2}^M + \frac{\partial \psi_{k2}^M}{\partial \theta}\omega - u_{k2}\right) +$$
$$+ \sum_{j=1}^{m} \frac{\partial T_j^M}{\partial \theta}\omega + \frac{\partial T_f^M}{\partial i_f^M} \cdot v_f \tag{4}$$

$$v_f = \frac{di_f^M}{dt} \tag{5}$$

$$G_{k1}^M = \frac{\partial T_{k1}^M}{\partial i_{k1}^M} \cdot \left(\frac{\partial \psi_{k1}^M}{\partial i_{k1}^M}\right)^{-1} \tag{6}$$

$$f_l^M = -\left(\frac{\partial \psi_l^M}{\partial i_l^M}\right)^{-1} \cdot \left(R^M i_l^M + \frac{\partial \psi_l^M}{\partial \theta}\omega\right), \quad l \in \{k2, f\} \tag{7}$$

$$g_l^M = \left(\frac{\partial \psi_l^M}{\partial i_l^M}\right)^{-1}, \quad l \in \{k2, f\} \tag{8}$$

where the indices k1, k2 and f denote the phases that produce the strong, rising, and falling components of phase current, respectively; u_{k1}, u_{k2} and u_f are the respective controls of phase-k1, k2 and f; $u_{k2} = V_{max}$; the superscript M denotes the model; i_n^M, ψ_n^M, and T_n^M ($n \in \{k1, k2, f\}$) are the current, flux linkage and phase torque of phase-n; T_e^M is the total torque; R^M is the stator winding resistance in each phase; θ and ω are the angular position and velocity of the rotor.

3.2 Nonlinear IMC for total torque

Due to the plant-model mismatch and various uncertainties, the plant output inevitably deviates from the model output.

Let y_{Te}^P be the torque output of the plant, i.e., $y_{Te}^P = T_e^P$, and e_{Te}^{PM} be the plant-model output error. Then,

$$e_{Te}^{PM} = y_{Te}^P - y_{Te}^M. \tag{9}$$

To improve the system's performance, the filter must be employed. For the first-order system as the subsystem (1), it can be selected as the following form

$$\begin{cases} \dot{x}_{Te}^F = -a_{Te}^F x_{Te}^E + a_{Te}^F e_{Te}^{PM} \\ y_{Te}^F = x_{Te}^F \end{cases} \qquad (10)$$

where the superscript F denotes the filter; a_{Te}^F is a positive real.

An auxiliary variable is defined as

$$y_{Te} = y_{Te}^m + y_{Te}^F - y_{Te}^* \qquad (11)$$

where y_{Te}^* is a desired trajectory that converges to a constant $\bar{y}_{Te}^*$. Our main control objective is to make the actual toque T_e^p tracks y_{Te}^* in spite of disturbances or plant-model mismatch.

According to the nonlinear IMC [8], the obtained control law can be written as

$$u_{k1} = -\frac{F_{k1}^M - a_{Te}^F x_{Te}^F + a_{Te}^F e_{Te}^{PM} - y_{Te}^* + a_{Te} y_{Te}}{G_{k1}^M} \qquad (12)$$

where a_{Te} is a positive real.

3.3 Nonlinear IMC for stator current of phase-f

Similar to that of the total torque, let y_f^p be the stator current output of phase-f in the plant, i.e., $y_f^p = i_f^p$, and e_f^{PM} be the plant-model current output error. Then,

$$e_f^{PM} = y_f^p - y_f^M. \qquad (13)$$

Corresponding with subsystem (3), the filter is selected as

$$\begin{cases} \dot{x}_f^F = -a_f^F x_f^F + a_f^F e_f^{PM} \\ y_f^F = x_f^F \end{cases} \qquad (14)$$

where a_f^F is a positive real.

The objective of the current controller is to force residual current i_f^p decay quickly to zero, besides achieve the stabilization of the stator current dynamics. When the desired decaying current trajectory is y_f^* that conveys to zero, an auxiliary variable is introduced as

$$y_f = y_f^M + y_f^F - y_f^*. \qquad (15)$$

On the basis of the nonlinear IMC, the current control law of phase-f can be calculated as

$$u_f = -\frac{f_f^M - a_f^F x_f^F + a_f^F e_f^{PM} - \dot{y}_f^* + a_f y_f}{g_f^M} \qquad (16)$$

where a_f is a positive real.

4 PROPERTIES

4.1 Convergence

For any positive real a_{Te}^F and a_f^F, which are large enough, given a_{Te} and a_f such that $a_{Te} > 0$ and $a_f > 0$. Then, the tracking errors of both torque and current will converge exponentially to zero in the nonlinear IMC-controlled SRM drive, in spite of the disturbances or plant-model mismatch.

The tracking error of torque is taken as an example to interpret them. As described in Section 3, the systems of the auxiliary variable y_{Te} is linearized as

$$\dot{y}_{Te} = -a_{Te} y_{Te}. \qquad (17)$$

Moreover, the tracking error of torque is written as

$$e_{Te}^P = y_{Te}^P - y_{Te}^* = y_{Te} + (a_{Te}^F)^{-1} \dot{x}_{Te}^F. \qquad (18)$$

If, $1/a_{Te}^F \approx 0$ then $e_{Te}^P \approx y_{Te}$. Thus, the auxiliary variable y_{Te} can be used to estimate the tracking error of the plant output torque. From (17) it can be obtained that y_{Te} will converge exponentially to zero if $a_{Te} > 0$.

The same interpretation can be applied to the tracking error of current.

4.2 Effects of control parameters

1) The control parameter a_{Te} has a direct effect on the dynamic, static performances and robustness of the closed-loop system, and it can be tuned to provide a compromise between the performances and robustness. No control action is taken in the limit as $a_{Te} \to 0$. On the contrary, the IMC controller (12) provides perfect control in the limit as $a_{Te} \to \infty$.

2) If the model is perfect, then the effect of the control parameter a_{Te} on the closed-loop response is particularly simple, large value results in vigorous responses, while small value causes sluggish responses. If $a_{Te} > 0$ and y_{Te}^* is bounded, the torque produced by the plant is bounded.

3) For the control parameter, the similar results can be obtained in current control of phase-f. But it does not affect the dynamic and static performance of the torque response because the torque controller can compensate the effects.

4.3 Equilibrium points of the system

At the steady state, the stable equilibrium points of the closed-loop system are, respectively

$$(\bar{T}_e^P, \ \bar{T}_e^M, \ \bar{x}_{Te}^F) = (\bar{y}_{Te}^*, \ \bar{y}_{Te}^* - \bar{e}_{Te}^{PM}, \ \bar{e}_{Te}^{PM}) \qquad (19)$$

$$(\bar{i}_f^P, \ \bar{i}_f^M, \ \bar{x}_f^F) = (0, \ -\bar{e}_f^{PM}, \ \bar{e}_f^{PM}). \qquad (20)$$

It is clear that, $\bar{e}_{Te}^{PM}$ will not be equal to zero when there exists the plant-model mismatch. But, owing to the SRM's unipolar currents $\bar{e}_f^{PM}$ may equal to zero even if the plant and model is mismatched. The details are given as the follows:

1) If the theoretical equilibrium point of current i_f^M is greater than or equal to zero, Then its actual equilibrium point is identical to the theoretical results.

2) If the theoretical equilibrium point of current i_f^M is less than zero, Then its actual equilibrium point will be equal to zero due to being limited by $i_f^M \geq 0$. As a result, $\bar{e}_f^{PM} = 0$, and only i_f^M decay to zero more quickly than i_f^P.

4.4 Nonlinear IMC system

The schematic diagram of the nonlinear IMC structure for SRM is shown in Figure 2. The drive mainly consists of four sections, i.e., the actual SRM and its power converter, SRM model, the filters, and the nonlinear IMC controllers.

The actual plant torque T_e^P is calculated by using the measured phase currents $\mathbf{I}^P = [i_1^P, i_2^P, ..., i_m^P]$ and rotor position θ. The measured position and calculated speed as the time-varying parameters are directly fed back to the SRM model and the controllers. The SRM model runs in parallel with the plant, its currents $\mathbf{I}^M = [i_1^M, i_2^M, ..., i_m^M]$ are fed back to the controllers. Moreover, the SRM model output torque T_e^M and residual current i_f^M are compared with the corresponding outputs of the plant, and the differences are fed back through the filters, where $\mathbf{x}^F = [x_{Te}^F, x_f^F]$ are the outputs of the filters.
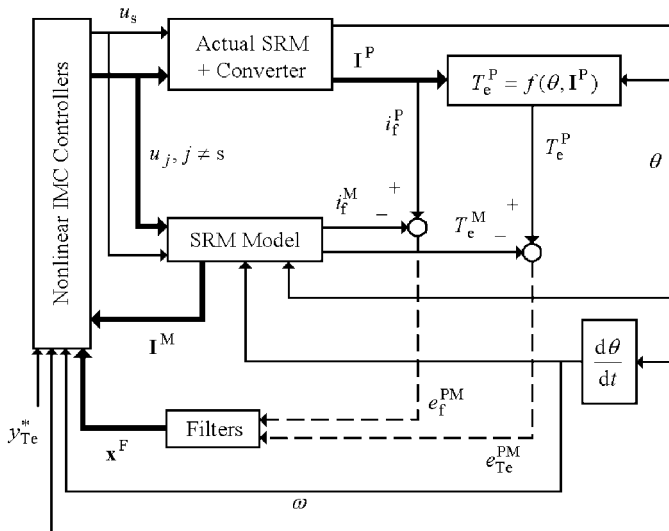

Fig. 2 Nonlinear IMC scheme of SRM drive

5 SIMULATION RESULTS

A SRM drive controlled by the nonlinear IMC controller as shown in Figure 2 has been simulated on an IBM PC using the software package MAT-LAB. The test motor is a four-phase 8/6-pole SRM and the details of its parameters are provided in the Appendix. The model suggested by Ilic'-Spong [3], which takes magnetic saturation into account, is used in this work. When using the phase inductance $L(\theta)$ at the phase current $i \approx 0$, unknown parameters a and b can be obtained, i.e., $a = 0.0545$ A^{-1}, and $b = 0.0454$ A^{-1}.

5.1 Dynamic and static performances

Figure 3 shows the dynamic responses of the torque developed by the plant when the nonlinear IMC-controlled SRM drive runs at a constant torque reference of 40 N·m. It can be seen that, the electromagnetic torque can quickly track the set point without any overshoot, and the compensation for the torque nonlinearity and torque ripple-free have been achieved by using the nonlinear IMC. The parameter a_{Te} directly affects the dynamics of the torque response, and the torque response is faster with a larger a_{Te}.
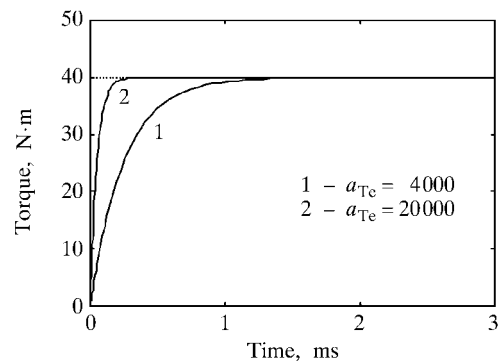

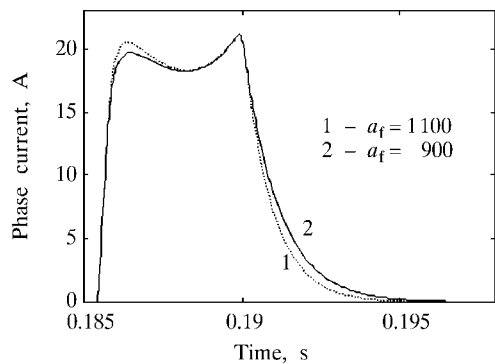*Fig. 3 Dynamic responses of torque produced by the plant*

Fig. 4 Current responses under the different a_f

Figure 4 shows the current responses of the SRM drive when the drive runs at the speed of 60 rad/s and the load torque of 30 N · m, where $\theta_{on} = 0.9$ and $\theta_c = 2$. It is clear that, the residual current decay more quickly to zero for the larger a_f, however, the rate of rise of current is correspondingly increased at the beginning of the conduction. But, the choice of a_f does not affect the dynamic and static performances of the torque response. It only affects the choice of turn-on angle θ_{on}.

5.2 Robustness

Robustness tests are carried out by varying the model parameters such as b (that is used to model the phase inductance), R^M, and ψ_s^M from their original values.
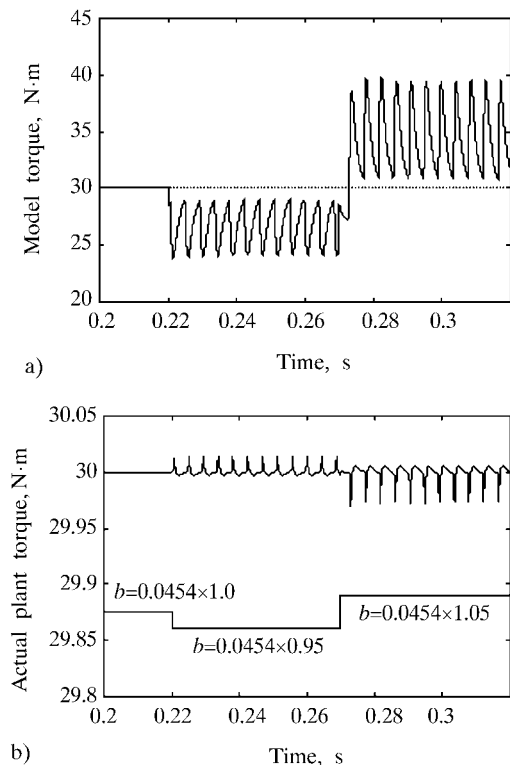
Fig. 5 Torque responses of the proposed drive under varying model parameter b

Figure 5 shows the torque responses of the nonlinear IMC-controlled SRM drive when the parameter b is varied by ±5 % from its original value, while the other parameters are held constant. Figures 6–7 show the corresponding torque responses when the model's saturated flux linkage ψ_s^M and phase resistance R^M are varied by ±20 % from the original value, respectively. Figures 8–10 show their respective current responses corresponding to Figures 5–7. The SRM drive runs at the speed of 60 rad/s and the load torque of 30 N · m.
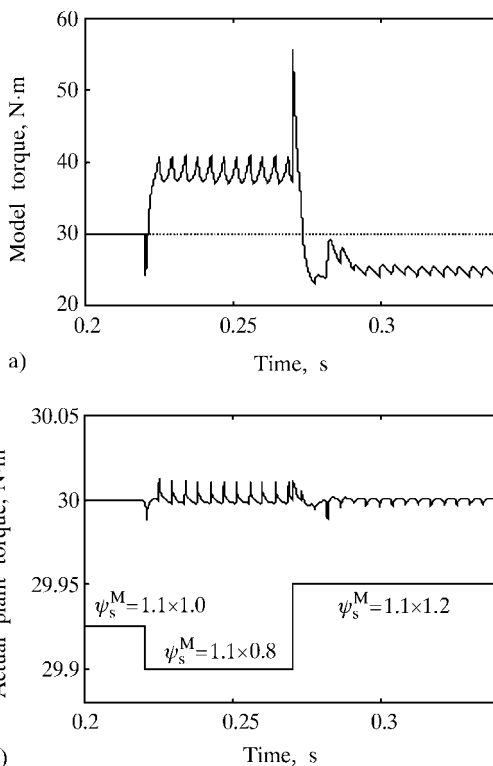
Fig. 6 Torque responses of the proposed drive under varying model parameter ψ_s^M

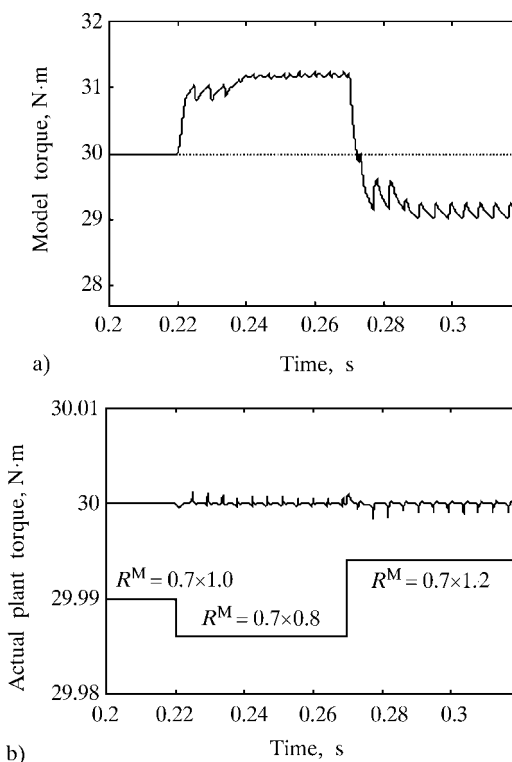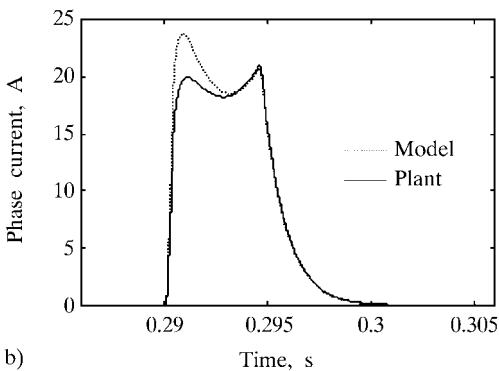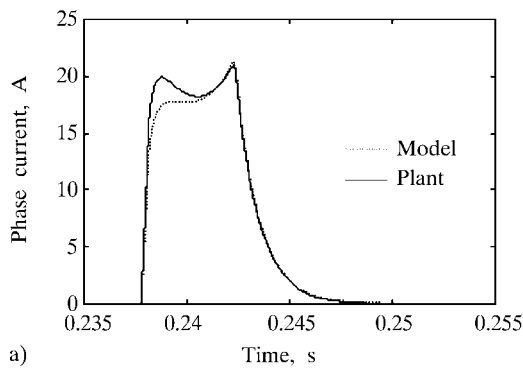Fig 7 Torque responses of the proposed drive under varying model parameter R^M

Fig. 8 Current responses under varying the model parameter b.
(a) b = 0.0454 × 0.95 A⁻¹, (b) b = 0.0454 × 1.05 A⁻¹.

Fig. 9 Current responses under varying the model parameter ψ_s^M.
(a) $\psi_s^M = 1.1 \times 0.8$ Wb, (b) $\psi_s^M = 1.1 \times 1.2$ Wb
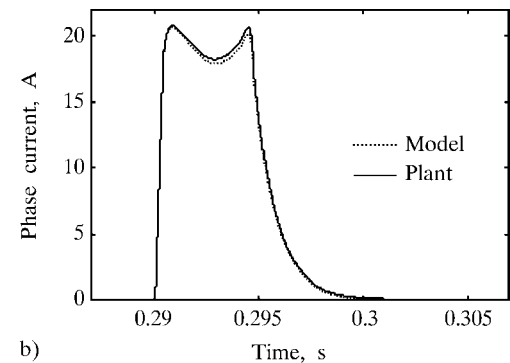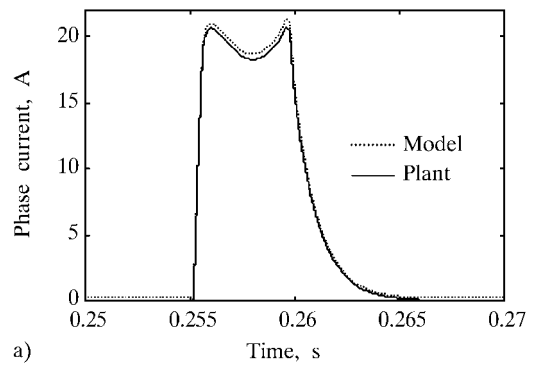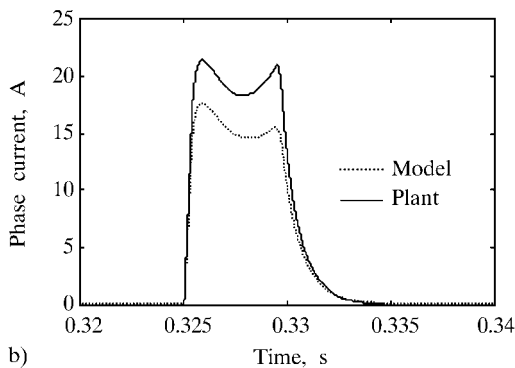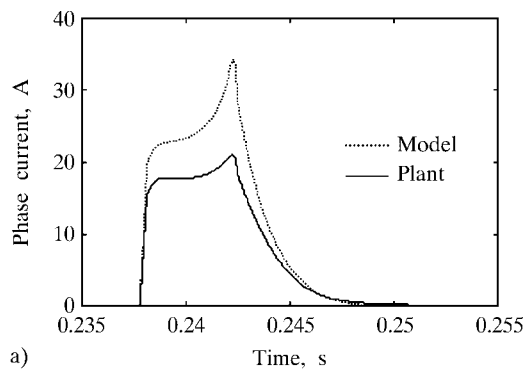

Fig. 10 Current responses under varying the model parameter R^M.
(a) $R^M = 0.7 \times 0.8$ Ω, (b) $R^M = 0.7 \times 1.2$ Ω

It can be seen in Figures 5–7 that the parameter variations have little effect on the torque produced by the plant although the torque ripple of the model gets significant, and the plant torque keeps the desired torque with very little ripple. It shows that the nonlinear IMC controller is highly robust against the parameter variations.

Moreover, as shown in Figures 8–10 the residual current of phase-off in the SRM model cannot always decay to zero when the model parameters are varied, and its equilibrium point is greater than or equal to zero. In the latter case, the residual current in the model decays more quickly than one of the plant. But, in any cases, the residual current of phase-off in the plant always decays quickly to zero. For example, in Figure 10 (a) a decreased R^M causes the model current higher than that of the plant. With the same decay rate, the plant current drops to zero firstly and after that the current controller sets zero to the decay rate of the model current so that it keeps at a small value above zero even in the afterward steady state. In the opposition, in Figure 10 (b) an increased R^M makes the model current lower than the plant one, thus it decays to zero earlier.
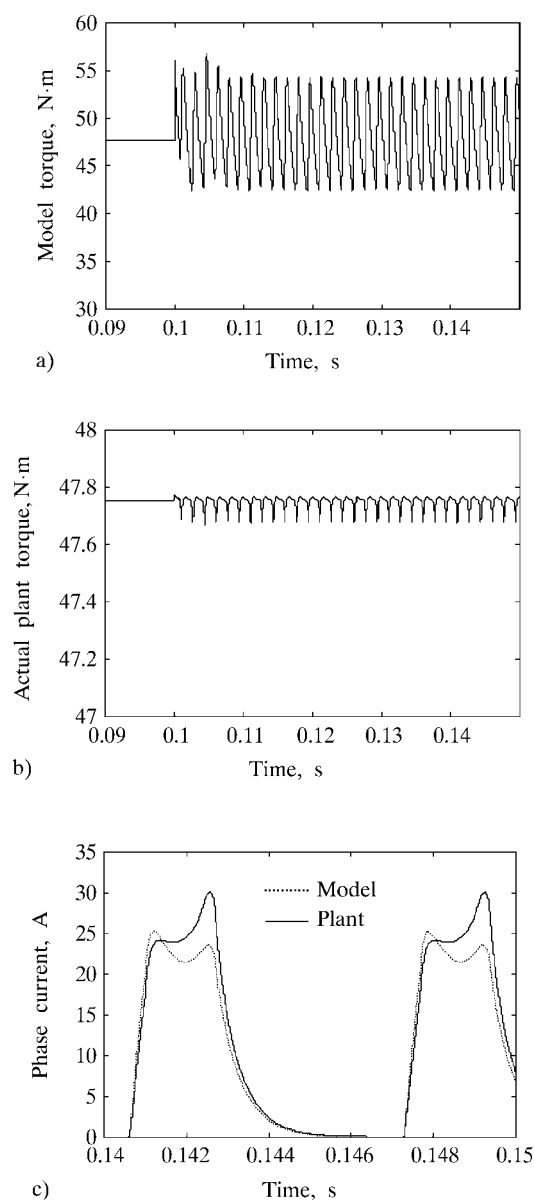
a)

b)

c)

Fig. 11 Torque and current responses of the proposed drive operating at 157 rad/s and 47.75 N·m

Figure 11 shows the responses of the torque and the phase current to the increases of R^M by 20 %, b by 5 %, and ψ_s^M by 10 % from their original values that match those plant ones, where the control system operates at the nominal speed 157 rad/s and nominal torque 47.75 N·m. From 0.09 s to 0.1 s the model matches the plant perfectly, afterward the model parameters increase. As a result, the model torque ripples are significant in Figure 11 (a). However, the plant torque keeps the balanced value with very small ripple limited to a band of ±0.2 % about mean, as shown in Figure 11 (b).

Anyway, the torque controller can effectively suppress the torque ripple. Moreover, increasing the value of a_{Te} can further reduce the ripple of the plant torque.

6 CONCLUSIONS

Based on the suitable commutation strategy proposed to compensate for the effects of the phase voltage saturation, the nonlinear IMC was applied to the SRM drive, and an effective SRM control method has been proposed to improve the overall performance of the drive. The important properties of the nonlinear IMC-controlled SRM drive such as its convergence, equilibrium points and effects of the control parameters on the system's performance were analyzed in detail. The results show that a plant-model mismatch can be tolerated in the drive, and the plant output will converge exponentially to the reference in spite of the disturbances or uncertainties. In addition, the torque control parameter has a direct effect on closed-loop performance, and the large values result in vigorous responses, while the small values cause sluggish responses. However, the current control parameter does not affect the dynamics and static state of torque response, and it only achieves stability task and affects the choice of turn-on angle in the commutation strategy.

The simulation tests carried out on a 7.5 kW four-phase SRM controlled by the nonlinear IMC have verified our novel control solution and its properties. The results proved that the nonlinear IMC has completely compensated for the nonlinear torque characteristics even if there is a plant-model mismatch. A dramatic reduction in torque ripple and the insensitivity of the responses of the nonlinear IMC-controlled drive to parameter variations and disturbances have been achieved.

APPENDIX

The parameters of SRM:

Rated power	7.5 kW
Rated voltage	460 V
Stator winding resistance	0.7 Ω
Stator/rotor poles	8/6
Phases	4
Rated speed	157 rad/s
Rated torque	47.75 N·m
Maximum inductance	110 mH
Minimum inductance	10 mH

REFERENCES

[1] J. Ish-Shalom, D. G. Manzer, **Commutation and Control of Step Motors.** Proc. 14th Symp. Incremental Motion, Contr. Syst. and Devices, pp. 283–292, June 1985.

[2] B. K. Bose, T. J. E. Miller, P. M. Szczesny, W. H. Bicknell, **Microcomputer Control of Switched Reluctance Motor.** IEEE Trans. Ind. Applicat., vol. IA-22, no. 4, pp. 708–715, Aug. 1986.

[3] M. Ilic'-Spong, R. Marino, S. M. Peresada, D. G. Taylor, **Feedback Linearizing Control of Switched Reluctance Motors.** IEEE Trans. Automat. Contr., vol. AC-32, no. 5, pp. 371–379, May 1987.

[4] S. K. Panda, P. K. Dash, **Application of Nonlinear Control to Switched Reluctance Motors: a Feedback Linearisation Approach.** IEE Proc.-Electr. Power Appl., vol. 143, no. 5, pp. 371–379, Sept. 1996.

[5] H. Cailleux, B. Le Pioufle, B. Multon, **Comparison of Control Strategies to Minimize the Torque Ripple of a Switched Reluctance Machine.** Electric Machines and Power Systems, vol. 25, no. 10, pp. 1103–1118, Dec. 1997.

[6] Y. Haiqing, S. K. Panda, L. Y. Chii, **Performance Comparison of Feedback Linearization Control with PI Control for Four-Quadrant Operation of Switched Reluctance Motors.** Proc. IEEE Appl. Power Electron. Conf. and Expo. (APEC), pp. 956–962, 1996.

[7] M. A. Henson, D. E. Seborg, **An Internal Model Control Strategy for Nonlinear Systems.** AIChE Journal, vol. 37, no. 7, pp. 1065–1081, Jul. 1991.

[8] J. Alvarez, S. Zazueta, **An Internal-Model Controller for a Class of Single-Input Single-Output Nonlinear Systems: Stability and Robustness.** Dynamics and Control, vol. 8, no. 2, pp. 123–144, Apr. 1998.

[9] R. S. Wallace, D. G. Taylor, **A Balanced Commutator for Switched Reluctance Motors to Reduce Torque Ripple.** IEEE Trans. Power Electron., vol. 7, no. 4, pp. 617–626, Oct. 1992.

[10] P. C. Kjaer, J. J. Gribble, T. J. E. Miller, **High-Grade Control of Switched Reluctance Machines.** IEEE Trans. Ind. Applicat., vol. 33, no. 6, pp. 1585–1593, Nov./Dec. 1997.

Nelinearno upravljanje s unutarnjim modelom za pogon s prekidačkim reluktantnim motorom bez oscilacija momenta. Predloženo je i razrađeno novo rješenje za upravljanje sklopnim reluktantnim motorom (SRM) zasnovano na nelinearnom upravljanju s unutarnjim modelom (IMC) i prikladnoj strategiji komutacije. Strategija komutacije koristi definiranu kritičnu poziciju rotora kao točku komutacije što doprinosi smanjenju računskih zahtjevnosti. Shema za upravljanje naponom SRM-a zasnovana na nelinearnom IMC-u osigurava linearizaciju zatvorenog sustava i robusnost IMC strukture što rezultira ukupnom robusnošću pogona bez oscilacija momenta unatoč nepodudaranju modela smetnji sa stvarnim smetnjama. Opisana su neka važna svojstva ovoga načina upravljanja. Simulacijskim se rezultatima pokazuje visoka kvaliteta upravljanja SRM-a.

Ključne riječi: nelinearno upravljanje s unutarnjim modelom, SRM, minimizacija oscilacija momenta

AUTHORS' ADDRESSES:

Dr. GE Baoming
Electrical Machinery Group,
Department of Electrical Engineering,
Tsinghua University, Beijing 100084,
P.R.China

Prof. WANG Xiangheng
Department of Electrical Engineering,
Tsinghua University, Beijing 100084,
P.R.China

Prof. JIANG Jingping
College of Electrical Engineering,
Zhejiang University, Huangzhou 310027,
P.R. China